Plant Physiol. (1992) 100, 733–739
0032-0889/92/100/0733/07/$01.00/0

Received for publication December 9, 1991
Accepted May 15, 1992

Effects of Water-Deficit Stress on Photosynthesis, Its Components and Component Limitations, and on Water Use Efficiency in Wheat (*Triticum aestivum* L.)[1]

Bjorn Martin* and Norma A. Ruiz-Torres

Department of Agronomy, Oklahoma State University, Stillwater, Oklahoma 74078–0507

ABSTRACT

It is of theoretical as well as practical interest to identify the components of the photosynthetic machinery that govern variability in photosynthesis rate (A) and water-use efficiency (WUE), and to define the extent by which the component processes limit A and WUE during developing water-deficit stress. For that purpose, leaf exchange of CO_2 and H_2O was determined in two growth-chamber-grown wheat cultivars (*Triticum aestivum* L. cv TAM W-101 and cv Sturdy), and the capacity of A was determined and broken down into carboxylation efficiency (c.e.), light- and CO_2-saturated A, and stomatal conductance (g_s) components. The limitations on A measured at ambient CO_2 concentration (A_{350}) were estimated. No cultivar difference was observed when A_{350} was plotted versus leaf water potential (Ψ_w). Light- and CO_2-saturated A, c.e., and g_s decreased with decreasing leaf Ψ_w, but of the corresponding photosynthesis limitations only those caused by insufficient c.e. and g_s increased. Thus, reduced stomatal aperture and Calvin cycle activity, but not electron transport/photophosphorylation, appeared to be major reasons for drought stress-induced inhibition of A_{350}. WUE measured as A_{350}/g_s first increased with stomatal closure down to a g_s of about 0.25 mol H_2O m^{-2} s^{-1} (Ψ_w = −1.6 MPa). However, it was predicted that A_{350}/g_s would decrease with more severe stress due to inhibition of c.e.

Large agricultural yield improvements have been achieved in many crops and environments over the last several decades (2). Improved pest control and field management practices, modified plant architecture, and altered harvest index have been keys to the success. However, these strategies have to date been largely exhausted, so further substantial improvements will require manipulation of basic biochemical and physiological processes.

The link between dry matter gain and water use is strong (2) and resides in the exchange of CO_2 for water at the leaf level (5). Significant genetically controlled variability in WUE[2] has been demonstrated among species as well as among cultivars within species, and experimental evidence suggests that WUE is stably inherited (13, 15). Farquhar and Richards (7) and Condon et al. (4) demonstrated potentially useful variability in WUE among wheat cultivars. Martin and Thorstenson (20) noted substantial variation in WUE among tomato genotypes and Martin et al. (19) were able to identify three restriction fragment-length polymorphisms markers that explained some 70% of the variation in WUE in their tomato population. To date, this remains the only report identifying discrete genomic locations that are of importance to plant WUE.

Both stomatal and nonstomatal factors are thought to contribute to drought effects on A (3, 21) and WUE. Yet it is largely unknown precisely what these processes are in terms of major biochemical, physiological, and/or anatomical mechanisms and traits, and exactly how they conspire to confer greater A and long-term WUE in any given plant and environment. However, it is clear that stomatal behavior is important because variation in g_s affects E proportionally more than A (E increases linearly with g_s, whereas A levels off at high g_s values). Another plausible mechanism for increased WUE is improved mesophyll capacity for photosynthesis, which allows A to increase and leaves E unaffected (8). The high capacity of mesophyll photosynthesis may result from optimum leaf anatomy minimizing the residual diffusive resistance or from having more (or more efficient) photosynthetic machinery per unit of projected leaf area (1). Greater Calvin cycle capacity is revealed by greater c.e., whereas greater steady-state capacity for photosynthetic electron transport and/or photophosphorylation is revealed by greater A_{max}.

In this study, we measured photosynthetic gas exchange of 5-week-old unvernalized wheat (*Triticum aestivum* L.) to determine the change in capacities of photosynthetic components during developing water-deficit stress. The objective was to identify mechanisms that limit A and restrict WUE in the hope that insight into the mechanisms will eventually aid in the logical manipulation of key traits so that future crops of superior productivity and WUE may be developed. We selected a method to estimate partial photosynthesis limitations that can be easily adapted to modeling and prediction of photosynthesis gains obtainable by finite, defined increases in g_s, c.e., and A_{max} alone or in combination. Two hard red winter wheat cultivars were used; cv TAM W-101

[1] This is journal article No. J-6139 of the Oklahoma Agricultural Experiment Station, Oklahoma State University, Stillwater, OK 74078.

[2] Abbreviations: WUE, water use efficiency; A, rate of net photosynthesis; C_i, intercellular CO_2 concentration; c.e., initial slope of A/C_i curve (carboxylation efficiency); subscripts *350* and *max*, measurements performed at 350 μL L^{-1} and saturating CO_2 concentrations, respectively; A_{max}, light- and CO_2-saturated rate of photosynthesis; E, rate of transpiration; g_s, stomatal conductance (for CO_2 unless otherwise stated); l_{gs}, l_{ce}, and l_{Amax}, reductions of A_{350} due to finite and limiting g_s, c.e., and A_{max}, respectively; Ψ_w, water potential.

has been reported to have greater A and drought resistance than cv Sturdy (16, 17, 22, 23).

MATERIALS AND METHODS

Plant Growth Conditions and Stress Exposure

Seeds of hard red winter wheat (*Triticum aestivum* L. cv TAM W-101 and cv Sturdy) were allowed to imbibe on moistened filter paper in Petri dishes. After 2 d, four seeds were placed in pots holding 1.3 L of a mixture of 1:1:3 (v/v/v) peat moss:vermiculite:top soil. The pots were placed in a growth chamber (Sherer Controlled Environment Chamber, model CEL 25-7 HL, Sherer-Gillett Co., Marshall, MI) maintained at 25/18°C day/night temperature. The photoperiod was 14 h and the irradiance at plant height was 500 μmol m^{-2} s^{-1} PAR, generated by a combination of fluorescent tubes and incandescent bulbs. The humidity was not controlled and varied between 30 and 60% RH. The pots were watered every other morning with Peters 20-20-20 (W.R. Grace & Co., Allentown, PA). After 1 week the seedlings were thinned to one per pot.

Exposure to water-deficit stress was achieved by withholding water after the morning of the first day of measurement.

Gas-Exchange Measurements

CO_2 Uptake

Steady-state gas-exchange rates of young, expanded, attached leaves were measured at light saturation (1800 μmol m^{-2} s^{-1} PAR) with a gas-exchange system described in detail by Johnson et al. (16). Briefly, on each day a plant was brought from the photophase of the growth chamber to the laboratory, and an attached leaf was sealed in a stirred assimilation chamber controlled at 25°C air temperature. Chamber humidity was measured with a condensation dew point hygrometer (System 1100DP, General Eastern Instruments Corp., Watertown, MA) and CO_2 concentration with an IR gas analyzer (PIR 2000 R, Horiba Instrument, Inc., Irvine, CA). Dry (dew point < −15°C), CO_2-free air from a compressed air cylinder was mixed with dry air from a second cylinder containing 1700 μL L^{-1} of CO_2. The mixing ratio and flow rate were varied to generate a range of CO_2 concentrations in the assimilation chamber. Corresponding C_is were computed as described by von Caemmerer and Farquhar (28). To speed up gas-exchange measurements, ambient humidity in the chamber was allowed to vary in the range of 50 ± 5% RH. The CO_2 fixation rate was first measured at the lowest CO_2 concentration and then in order of increasing CO_2 concentration. Steady-state rates were usually obtained within 20 min, but occasionally longer equilibration times were required in the most stressed plants. The calculated C_is were plotted against measured A values to produce photosynthetic C_i response curves (A/C_i curves).

A concentration of 350 μL CO_2 L^{-1} of air was considered normal ambient CO_2 concentration (C_a). This C_a was included in all CO_2 response curves, allowing A in ambient air, A_{350}, to be obtained and g_s (the photosynthetic supply function, Farquhar and Sharkey [8]) to be graphed as in Figure 1. The greatest A measured on a given day was used as the A_{max}. g_s was computed according to standard procedures (28). c.e. was calculated as the slope of the linear phase at low C_i of the A/C_i curve. Because, for reasons mentioned above, ambient humidity was allowed to vary somewhat, the instantaneous leaf WUE was calculated as A_{350}/g_s.

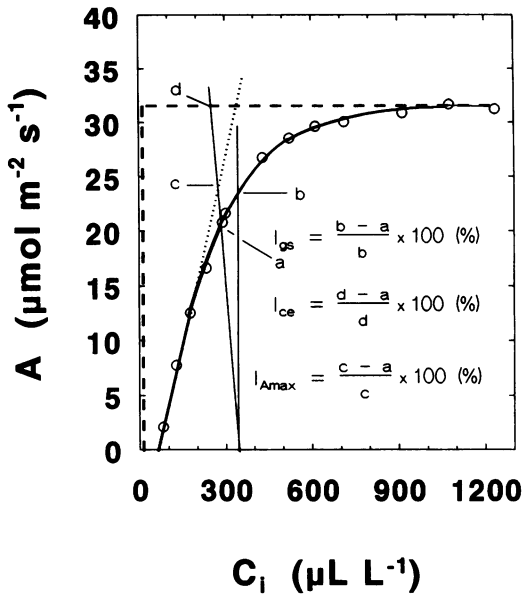

Figure 1. Illustration of the dependence of A on C_i and definition of computations of the partial photosynthesis limitations l_{gs}, l_{ce}, and l_{Amax}. Solid A/C_i curve, Observed photosynthetic demand function; dashed line, idealized photosynthetic demand function assuming infinite c.e.; dotted line, idealized photosynthetic demand function assuming infinite A_{max}; thin solid line (negative slope), observed photosynthetic supply function (g_s); thin solid line (parallel to *y* axis), photosynthetic supply function assuming infinite g_s; a, A_{350}; b, A at infinite g_s; c, A at intersect of supply function and idealized demand function assuming infinite A_{max}; d, A at intersect of supply function and idealized demand function assuming infinite c.e. (for more detail see "Materials and Methods").

Figure 1 illustrates calculation of stomatal limitation as described by Farquhar and Sharkey (8) and Sharkey (24), and analogous calculations of the mesophyll limitations caused by insufficient c.e. (traditionally interpreted in terms of Rubisco activity, but now considered to involve the activity of the entire Calvin cycle), l_{ce}, and by insufficient A_{max} (thought to reflect steady-state electron transport and/or photophosphorylation capacity), l_{Amax}. The l_{gs} was calculated as $[(b - a)/b] \times 100$, thus comparing the plant under study with a theoretical plant with identical c.e. and A_{max} but with infinite g_s (zero stomatal limitation). Similarly, l_{ce} ($[(d - a)/d] \times 100$) compares the studied plant with a theoretical plant having identical g_s and A_{max} but with infinite c.e. (the reference plant has no oxygenase activity and no resistance between the intercellular air space and the site of carboxylation in the chloroplast). The l_{Amax} ($[(c - a)/c] \times 100$) compares the studied plant with a plant having identical g_s and c.e. but infinitely great A_{max}. Thus, l_{gs}, l_{ce}, and l_{Amax} are percentage estimates of reductions in A_{350} caused by finite and limiting g_s, c.e., and A_{max}, respectively.

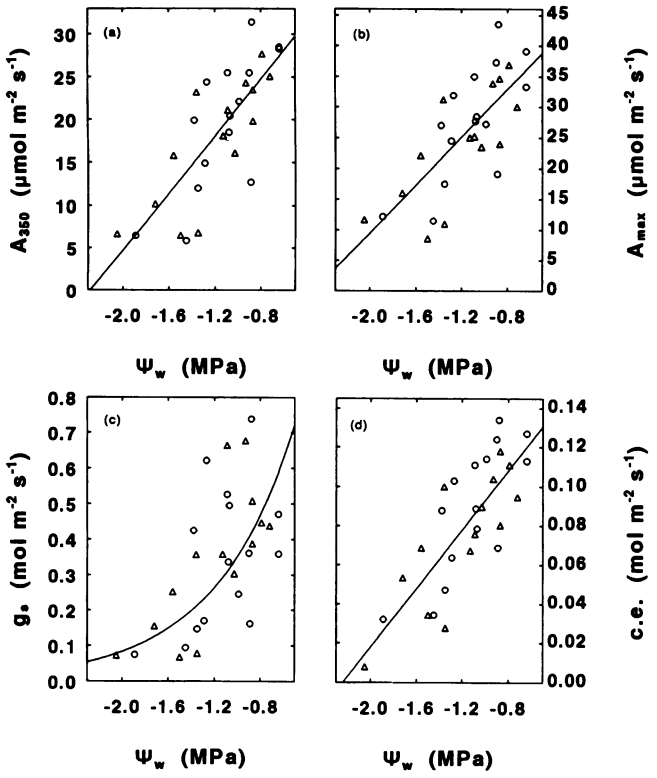

Figure 2. Dependencies on leaf Ψ_w of (a) A_{350}; (b) A_{max}; (c) g_s; and (d) c.e. O, cv TAM W-1-1; Δ, cv Sturdy. $A_{350} = 38.12 + 16.71 \times \Psi_w$, $r = 0.78$, $P < 0.01$; $A_{max} = 48.58 + 19.53 \times \Psi_w$, $r = 0.74$, $P < 0.01$; ln g_s = ln $1.479 + 1.436 \times \Psi_w$, $r = 0.70$, $P < 0.01$; c.e. $= 0.168 + 0.075 \times \Psi_w$, $r = 0.80$, $P < 0.01$. Six plants (three of each cultivar) were used. Each data point is for a different leaf on a different tiller.

All measurements were made on the last day of watering and during the following 4 d.

O_2 Evolution

Rates of photosynthetic O_2 evolution of excised wheat leaves were measured at 25°C with a leaf disc electrode (Hansatech Ltd., King's Lynn, England) operated at 5% CO_2 in the air (29). Light-saturated rates were determined at 1650 μmol m^{-2} s^{-1} PAR. Apparent quantum yields were determined by calculating the slope of the linear regression of the plot of O_2 evolution versus incident PAR at low irradiance. Five irradiances below 110 μmol m^{-2} s^{-1} PAR were obtained with combinations of neutral density filters (Ealing-Electro Optics, Inc., Holliston, MA).

Measurements of light-saturated O_2 evolution rates were made on the last day of watering and on the following 4 d. The apparent quantum yield of O_2 evolution was determined in a separate experiment on the last day of watering and intermittently during the next 7 d.

Determination of Leaf Ψ_w

At the time of leaf detachment, leaf samples were collected from test leaves for determination of leaf Ψ_w using leaf cutter psychrometers (J.R.D. Morrill Specialty Equipment, Logan, UT) connected to an HP-115 water potential measurement system (Wescor Inc., Logan, UT). Reported Ψ_w values are averages of two 0.31-cm^2 leaf discs determined after 2 h of equilibration of the psychrometers in a water bath at 30°C.

Data presented in figures were tested for linear, logarithmic, exponential, and second-order polynomial fits, and best fit regressions were selected.

RESULTS

There was no cultivar difference between *T. aestivum* cv TAM W-101 and cv Sturdy when A_{350} was compared at identical leaf Ψ_w (Fig. 2a). Therefore, the regression of A_{350} on Ψ_w is based on all data points (also, all of the following regressions are based on combined cultivar data). As decreasing leaf Ψ_w reduced A_{350}, A_{max} (Fig. 2b), g_s (Fig. 2c), and c.e. (Fig. 2d) also decreased. A_{350}, A_{max}, and c.e. showed linear relationships with Ψ_w, whereas a logarithmic transformation better described the relationship between g_s and Ψ_w ($r = 0.60$ for the linear regression of g_s on Ψ_w, whereas $r = 0.70$ for the logarithmic transformation). Water stress that reduced Ψ_w from −0.84 MPa (average of unstressed plants) to −2.00 MPa reduced A_{350} from 24.1 to 4.7 μmol CO_2 m^{-2} s^{-1} (5.1-fold), A_{max} from 32.2 to 9.5 μmol CO_2 m^{-2} s^{-1} (3.8-fold), c.e. from 0.105 to 0.018 mol CO_2 m^{-2} s^{-1} (5.8-fold), and g_s from 0.443 to 0.084 mol CO_2 m^{-2} s^{-1} (5.3-fold). The regression equation in the legend of Figure 2a predicts A_{350} to reach zero at $\Psi_w = -2.28$ MPa. At this Ψ_w, c.e. was also zero (Fig. 2d), while about 10% of A_{max} (Fig. 2b) and g_s (Fig. 2c) remained.

Figure 3 shows the relationship between leaf Ψ_w and computed values of partial photosynthesis limitations. The l_{gs} (Fig. 3a) and l_{ce} (Fig. 3b) increased linearly with drought-induced reduction in Ψ_w, whereas l_{Amax} (Fig. 3c) decreased with lowered Ψ_w. Again comparing a severely stressed plant at $\Psi_w = -2.00$ MPa with a control plant at −0.84 MPa, l_{gs} increased with the stress from 9.4 to 23.2% (2.5-fold) and l_{ce} from 22.1 to 41.5% (1.9-fold), resulting in an increase of about 40% in the ratio of l_{gs}/l_{ce}. The l_{Amax} decreased dramatically from 8.1% to near zero within the same Ψ_w range.

The relationships between A_{350} and magnitude of the partial photosynthetic limitations are presented in Figure 4. A_{350} decreased linearly with the increase in two of the partial limitations, l_{gs} (Fig. 4a) and l_{ce} (Fig. 4b). A_{350} was not significantly correlated with the third partial limitation, l_{Amax} (Fig. 4c).

Figure 5 illustrates how WUE expressed as A_{350}/g_s varied over a range of g_s values, when g_s was reduced by withholding of water. The line in the figure describes the predicted variation in A_{350}/g_s over a range of g_s values utilizing the regression equations for A_{350} and g_s (see legend of Fig. 2, a and c) to calculate the magnitude of each parameter. The curve shows an initial increase in A_{350}/g_s when g_s decreased. After A_{350}/g_s peaked slightly below $g_s = 0.25$ mol H_2O m^{-2} s^{-1} ($\Psi_w = -1.6$ MPa), the ratio precipitously decreased with a further decrease in g_s. The collected data points agree well with the calculated dependence of A_{350}/g_s on g_s at $g_s > 0.25$ mol m^{-2} s^{-1}. The plants we used were not sufficiently stressed to test experimentally the precipitous drop in A_{350}/g_s predicted in severely stressed plants at very low g_s.

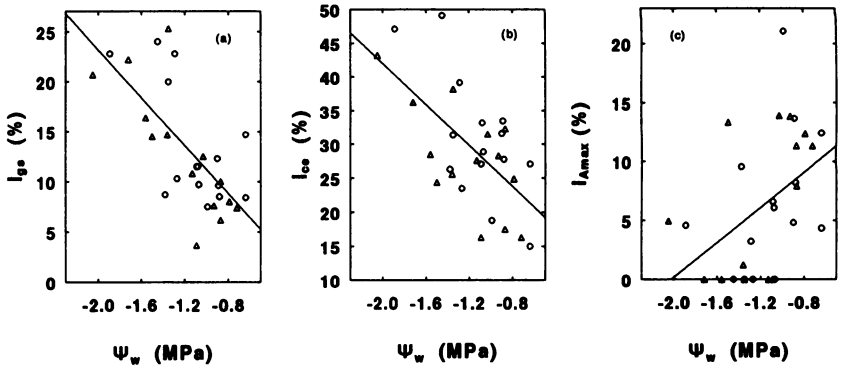

Figure 3. Dependencies on leaf Ψ_w of (a) I_{gs}; (b) I_{ce}; and (c) I_{Amax}. O, cv TAM W-101; Δ, cv Sturdy. $I_{gs} = -0.76 - 11.97 \times \Psi_w$, $r = -0.70$, $P < 0.01$; $I_{ce} = 8.09 - 16.89 \times \Psi_w$, $r = -0.70$, $P < 0.01$; $I_{Amax} = 14.98 + 7.40 \times \Psi_w$, $r = 0.45$, $P < 0.05$. Six plants (three of each cultivar) were used. Each data point is for a different leaf on a different tiller.

Two additional methods were employed to verify the presence of a nonstomatal component of the drought-induced inhibition of photosynthesis. First, A_{max} and A estimated from A/C_i curves at $C_i = C_a = 350$ μL L^{-1} of CO_2 were plotted against each other (Fig. 6). We observed a linear regression ($r = 0.98$) going through the origin, as expected if both were independent measures of photosynthesis unaffected by stomatal influences. Second, the photosynthetic O_2 evolution rate measured at 5% atmospheric CO_2 with a leaf disc electrode also decreased with decreasing leaf Ψ_w (Fig. 7). Both the light-saturated rate of photosynthetic O_2 evolution (Fig. 7a) and the apparent quantum yield for O_2 evolution (Fig. 7b) declined about 40% upon reduction of leaf Ψ_w from −0.84 to −2.00 MPa.

DISCUSSION

It has been previously reported that the mean photosynthesis rate of *T. aestivum* cv TAM W-101 was greater than the rate of cv Sturdy (16, 22). We also noted that the mean of the first cultivar was higher, but the difference was not statistically significant on any day of our experiment (values for unstressed control plants were $A_{350} = 28.5 \pm 3.0$ μmol m^{-2} s^{-1} [cv TAM W-101] and $A_{350} = 25.2 \pm 2.2$ μmol m^{-2} s^{-1} [cv Sturdy]).

Our data are in agreement with several reports on reduction by water stress of A_{350}, g_s, c.e., and A_{max} (14, 16, 18, 21, 22). It is interesting that in our study both components of the photosynthetic demand function (8), i.e. A_{max} (Fig. 2b) (a measure of steady-state chloroplast capacity to generate NADPH and/or ATP) and c.e. (Fig. 2d) (a measure of Calvin-cycle activity) decreased 4- to 6-fold with a reduction in leaf Ψ_w from −0.84 to −2.00 MPa, as did g_s (Fig. 2c), which represents the supply function. Because g_s was logarithmically related to Ψ_w (Fig. 2c) whereas c.e. showed a straight line relationship with Ψ_w (Fig. 2d), we calculated that g_s/c.e. first decreased somewhat down to $\Psi_w = -1.6$ MPa, but, with a further decline in Ψ_w, g_s/c.e. increased again and became infinitely great when c.e. approached zero at $\Psi_w = -2.28$ MPa. A_{max} decreased with decreasing Ψ_w somewhat less steeply so it extrapolated to zero first at $\Psi_w = -2.49$ MPa (Fig. 2b).

Therefore, although photosynthetic electron transport and/or photophosphorylation (A_{max}) capacity decreased with increasing water stress, the portion of this capacity that exceeded A_{350} increased relative to the magnitude of A_{350}. This conclusion was supported by calculating the regression of A_{max} on A_{350} ($A_{max} = 3.40 + 1.20 \times A_{350}$, $r = 0.98$; data not shown). Using this very strong linear correlation, we calculated that the fraction of A_{max} that was in excess of A_{350} increased from 43% at $\Psi_w = -0.84$ MPa to 103% at $\Psi_w = -2.00$ MPa, although both A_{max} and A_{350} declined. We conclude that impairment of electron transport and/or photophosphorylation, although it occurred, was not the reason for drought inhibition of A_{350}. Rather, the coincident decrease with leaf Ψ_w of A_{350} (Fig. 2a), g_s (Fig. 2c), and c.e. (Fig. 2d) suggests that closing of stomata and impairment of the Calvin cycle were fundamental to the decrease in A_{350}. The intercept with the x axis at about $\Psi_w = -2.28$ for both A_{350} and c.e suggests that drought inhibition of the Calvin cycle caused complete elimination of photosynthesis under severe stress. Heitholt et al. (14) reported that in vitro-activated Rubisco

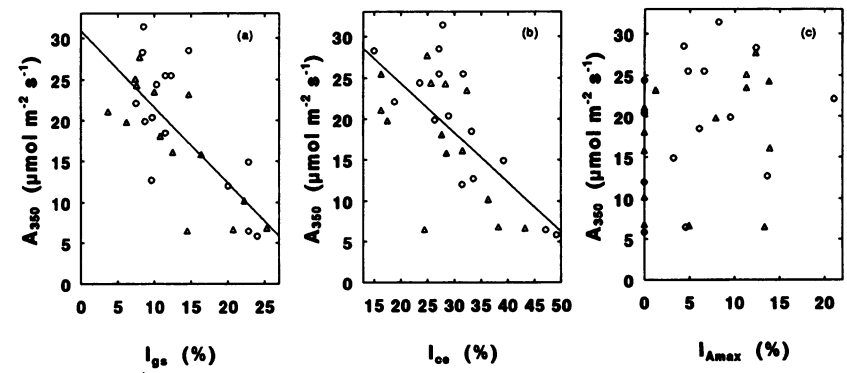

Figure 4. Dependencies of A_{350} on (a) I_{gs}; (b) I_{ce}; and (c) I_{Amax}. O, cv TAM W-101; Δ, cv Sturdy. $A_{350} = 30.91 - 0.93 \times I_{gs}$, $r = -0.74$, $P < 0.01$; $A_{350} = 36.05 - 0.63 \times I_{ce}$, $r = -0.70$, $P < 0.01$; $A_{350} = 16.37 + 0.36 \times I_{Amax}$, $r = 0.28$, not significant. Six plants (three of each cultivar) were used. Each data point is for a different leaf on a different tiller.

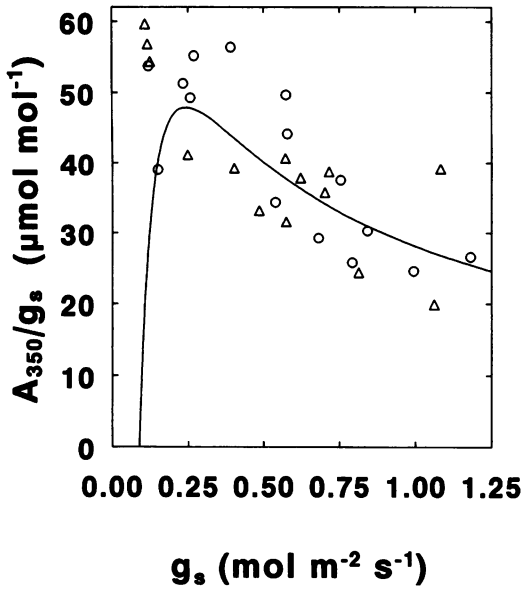

Figure 5. Dependency of WUE measured as A_{350}/g_s on g_s for water vapor. O and Δ, Observations on cv TAM W-101 and cv Sturdy, respectively. Curve represents prediction based on the regression equations of $A_{350} = f(\Psi_w)$ (Fig. 2a) and $g_s = f(\Psi_w)$ (Fig. 2c). Six plants (three of each cultivar) were used. Each data point is for a different leaf on a different tiller.

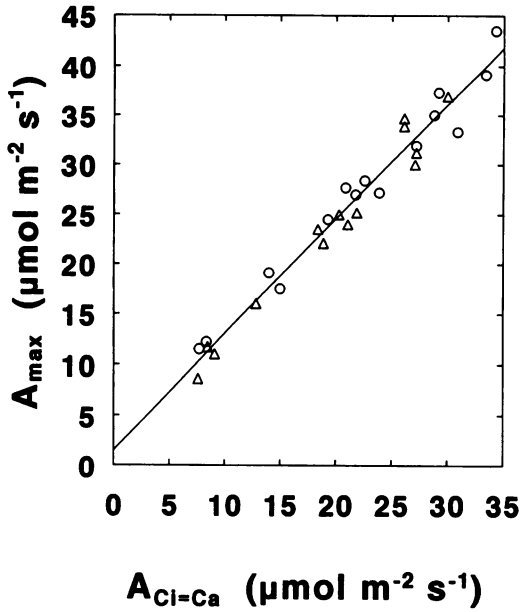

Figure 6. Dependence of A_{max} on A at $C_i = C_a = 350$ µL L^{-1} (from A/C_i curves). O, cv TAM W-101; Δ, cv Sturdy. $A_{max} = 1.486 + 1.153 \times A_{Ci=Ca}$, $r = 0.98$, $P < 0.01$. Six plants (three of each cultivar) were used. Each data point is for a different leaf on a different tiller.

activity decreased in drought-stressed wheat. However, the more relevant question remains to be answered, which is whether the in vivo activity of this enzyme also decreases, as is suggested by the initial slope of the A/C_i curve.

The conclusions described above were supported by calculation of values of partial photosynthesis limitations over a range of Ψ_w. The nonstomatal limitation was determined after partitioning it into a component dependent on c.e. (Calvin-cycle activity) and another component related to A_{max} (electron transport/photophosphorylation). Our computations of l_{ce} and l_{Amax} are analogous to the calculation of l_{gs} by Farquhar and Sharkey (8) but differs from Sharkey's (24) method to calculate a mesophyll limitation.

From Figure 2, c and d, and Figure 3, a and b, it is seen that while g_s and c.e. decreased as much as five to six times (over a range of Ψ_s from −0.84 to −2.00 MPa) their resultant limitations, l_{gs} and l_{ce}, increased, although to a lesser extent (2- to 3-fold). In control plants, the magnitude of the third partial limitation l_{Amax} was about 8% (making this the smallest partial limitation of the three), and it is interesting that this partial limitation decreased rather than increased with increasing severity of stress (Fig. 3c). Such a dependence of l_{Amax} on Ψ_w is consistent with the observation noted above that although A_{max} decreased with decreasing Ψ_w, the proportion of A_{max} that was in excess of the operating rate of net photosynthesis increased. Our conclusions are (a) that all three, g_s, ce, and A_{max}, colimited photosynthesis in unstressed wheat; and (b) that the magnitude of all three parameters decreased with decreasing Ψ_w; but (c) that only the limitations by stomata (l_{gs}) and insufficient carboxylation efficiency (l_{ce}) became greater under water stress.

It has been predicted that WUE measured as A/E will initially increase with stomatal closure due to greater reduction in E than in A, but that eventually leaf conductance will decrease to levels where insufficient heat and gas transfer will cause WUE to deteriorate (6). It is interesting that our findings of WUE expressed as A_{350}/g_s, which should not be affected by conduction inefficiencies, also suggested such a

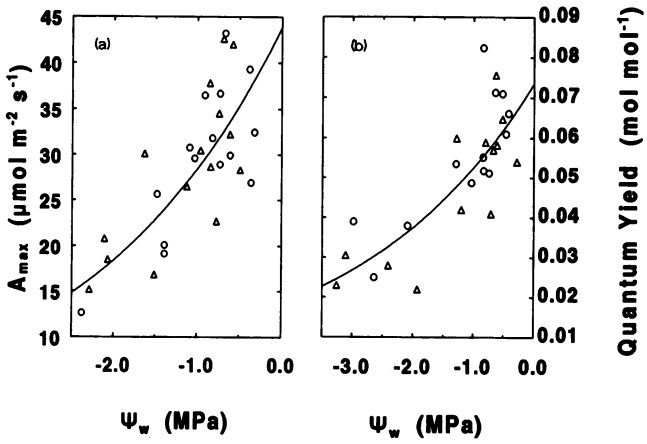

Figure 7. Dependence on leaf Ψ_w of (a) light-saturated O_2 evolution and (b) apparent quantum yield of O_2 evolution (QY). Measurements were made at 5% CO_2 with a Hansatech leaf disc electrode. O, cv Tam W-101; Δ, cv Sturdy. $\ln A_{max} = \ln 43.84 + 0.43 \times \Psi_w$, $r = 0.80$, $P < 0.01$; $\ln QY = \ln 0.074 + 0.337 \times \Psi_w$, $r = 0.83$, $P < 0.01$. Six plants (three of each cultivar) were used in determinations of A_{max}, and four plants (two of each cultivar) in determinations of quantum yield. Each data point is for a different leaf on a different tiller.

behavior (Fig. 5). This is consistent with the observation by Ritchie et al. (22) that A/g_s of wheat was lower on both sides of a maximum around 60 to 70% relative leaf water content. We conclude that A_{350}/g_s decreased at g_s below 0.25 mol H_2O m^{-2} s^{-1} ($\Psi_w = -1.6$ MPa) because c.e. already extrapolated to zero at $\Psi_w = -2.28$ MPa, at which Ψ_w a small but significant g_s still remained (Fig. 2). Thus, inhibition of mesophyll photosynthesis seemed to be responsible for the predicted drop in WUE at very low g_s. Gummuluru et al. (11) noted that WUE and C_i of durum wheat were positively correlated with stomatal resistance only in rewatered plants, not in stressed plants prior to rewatering. Furthermore, A recovered less than E upon rewatering. Condon et al. (4) estimated that variation in leaf conductance and in mesophyll photosynthetic capacity contributed about equally to the variation in intercellular/ambient partial pressure of CO_2 in wheat, so both components should govern variation in WUE also (7). These findings, as well as ours, suggest that nonstomatal inhibition of photosynthesis indeed contributes to reduced A and WUE under stress. Due to difficulties in making sufficiently precise gas-exchange measurements in plants with very small g_s, we did not attempt to verify experimentally the decline predicted in A_{350}/g_s at very low Ψ_w and small g_s.

Gunasekera and Berkowitz (12) used a short pulse of $^{14}CO_2$ exposure to conclude that even wheat severely and rapidly exposed to drought (down to $\Psi_w = -2.6$ MPa in a few days) responded by homogenous stomatal closure, unlike the patchy stomatal closure caused by drought in some other species and by ABA treatment in wheat. That nonstomatal inhibition of photosynthesis indeed occurred in our experiments was strongly corroborated by observations of about 40% drought inhibitions of the light-saturated rate of photosynthetic O_2 evolution (Fig. 7a) and of the apparent quantum yield (Fig. 7b) using a leaf disc electrode with 5% CO_2 in the air. Graan and Boyer (10) compared ABA and drought treatments of sunflower and showed that stomatal diffusive restrictions were overcome at much lower external CO_2 concentration than could overcome drought inhibition. They concluded that, rather than overcoming stomatal limitations, extreme CO_2 levels in the air (in the range of one to several percent) reduced mesophyll inhibition of photosynthesis. Based on this interpretation, the smaller extent of mesophyll inhibition in our experiments determined with the leaf disc electrode at 5% CO_2 (Fig. 7) than with the IR gas analysis equipment at lower external CO_2 concentration (Fig. 2b) may not be a result of stomatal effects but can be explained in terms of an impact of extreme CO_2 levels on mesophyll photosynthesis.

We further evaluated the possibilities of stomatal patchiness (and the resultant inability to accurately calculate C_i) and of lack of CO_2 saturation of the stomatal influence on A at the highest external CO_2 level used with the IR gas analysis equipment. We reasoned that if there were indeed neither stomatal patchiness nor lack of saturation, then the mesophyll capacity for photosynthesis could be estimated in two ways: (a) the rate of A measured at the plateau of the A/C_i curve at high CO_2 would be one estimate of mesophyll photosynthesis, and (b) A determined from the A/C_i curve at $C_i = C_a = 350$ μL L^{-1} would be another estimate. If these estimates were truly two independent reflections of the capacity of mesophyll photosynthesis, they should generate a straight line going through the origin of the graph when plotted against each other. Lack of saturation of the stomatal influence on A should underestimate A_{max} (y axis in Fig. 6), and the error should be more prominent the more closed the stomata are. Patchy stomata should underestimate A at $C_i = C_a$ (x axis in Fig. 6), and this type of error should be at a maximum at some intermediate g_s and A values (there should be little or no patchiness when stomata are either fully closed or fully open). Figure 6 shows a straight line that extrapolates closely through the origin. Also, there is no deviation from linearity in the low or intermediate range of photosynthesis rates. These observations support the notion that patchiness and lack of CO_2 saturation of any stomatal effects were not significant, but that, indeed, nonstomatal drought effects on photosynthesis were.

Questions have recently been raised for other reasons (26, 27) regarding the classic interpretation of A/C_i curves and the partitioning of photosynthesis inhibition into stomatal and nonstomatal components (8, 24). The concerns are based on current insights into the regulation of photosynthetic carbon metabolism and electron transport and the role sucrose phosphate synthase may play (9, 25). Vassey and coworkers (26, 27) have found evidence that low internal CO_2 concentration inhibits sucrose synthesis and leads to feedback inhibition of the biochemistry of photosynthesis. Recovery upon elevation of the CO_2 concentration appears slow following lengthy photosynthesis depression. If the dependence of Calvin-cycle activity and/or electron transport/photophosphorylation on internal CO_2 concentration and sucrose synthesis is verified, much terminology currently in common use, as well as the terminology used in this paper, may need to be modified. Then l_{gs}, l_{ce}, and l_{Amax} may all ultimately depend on stomata, l_{gs} directly and l_{ce} and l_{Amax} indirectly. One practical consequence may be that although manipulation of the regulation of Calvin-cycle enzymes and electron transport may individually affect drought increases in l_{ce} and l_{Amax}, respectively, manipulation of stomatal behavior alone, in addition to affecting l_{gs}, could also influence l_{ce} and l_{Amax}. Also, accumulating a greater amounts of the components of photosynthetic electron transport and more coupling factor would not necessarily increase A_{max} and reduce l_{Amax}, but altering the stomatal response or increasing the activity and drought tolerance of the rate-limiting step in sucrose synthesis, thought to be sucrose phosphate synthase, could have such a beneficial effect. These issues must be resolved before we can gain a complete understanding of how to interpret A/C_i curves and what the practical implications are of partitioning photosynthesis limitation into stomatal and mesophyll components.

LITERATURE CITED

1. **Austin RB, Morgan CL, Ford MA, Bhagwat SG** (1982) Flag leaf photosynthesis of *Triticum aestivum* and related diploid and tetraploid species. Ann Bot **49:** 177–189
2. **Boyer JS** (1982) Plant productivity and environment. Science **218:** 443–448
3. **Bunce JA** (1988) Nonstomatal inhibition of photosynthesis by water stress. Reduction in photosynthesis at high transpiration

rate without stomatal closure in field-grown tomato. Photosynth Res **18:** 357–362

4. **Condon AG, Farquhar GD, Richards RA** (1990) Genotypic variation in carbon isotope discrimination and transpiration efficiency in wheat. Leaf gas exchange and whole plant studies. Aust J Plant Physiol **17:** 9–22
5. **Cowan IR** (1982) Regulation of water use in relation to carbon gain in higher plants. *In* OL Lange, PS Nobel, CB Osmond, H Ziegler, eds, Encyclopedia of Plant Physiology. II. Water Relations and Carbon Assimilation, New Series, Vol 12B. Springer-Verlag, New York, pp 589–613
6. **Farquhar GD, Ehleringer JR, Hubick KT** (1989) Carbon isotope discrimination and photosynthesis. Annu Rev Plant Physiol **40:** 503–537
7. **Farquhar GD, Richards RA** (1984) Isotopic composition of carbon correlates with water-use efficiency of wheat genotypes. Aust J Plant Physiol **11:** 539–552
8. **Farquhar GD, Sharkey TD** (1982) Stomatal conductance and photosynthesis. Annu Rev Plant Physiol **33:** 317–345
9. **Foyer C, Furbank R, Harbinson J, Horton P** (1990) The mechanisms contributing to photosynthetic control of electron transport by carbon assimilation in leaves. Photosynth Res **25:** 83–100
10. **Graan T, Boyer JS** (1990) Very high CO_2 partially restores photosynthesis in sunflower at low water potentials. Planta **181:** 378–384
11. **Gummuluru S, Hobbs SLA, Jana S** (1989) Physiological responses of drought tolerant and drought susceptible durum wheat genotypes. Photosynthetica **23:** 479–485
12. **Gunasekera D, Berkowitz G** (1991) Evaluation of heterogenous stomatal closure in leaves of water stressed plants (abstract No. 740). Plant Physiol **96:** S-109
13. **Hall AE, Mutters RG, Hubick KT, Farquhar GD** (1990) Genotypic differences in carbon isotope discrimination by cowpea under wet and dry field conditions. Crop Sci **30:** 300–305
14. **Heitholt JJ, Johnson RC, Ferris DM** (1991) Stomatal limitation to carbon dioxide assimilation in nitrogen- and drought-stressed wheat. Crop Sci **31:** 135–139
15. **Hubick KT, Shorter R, Farquhar GD** (1988) Heritability and genotype × environment interactions of carbon isotope discrimination and transpiration efficiency in peanut (*Arachis hypogaea* L.). Aust J Plant Physiol **15:** 799–813
16. **Johnson RC, Kebede H, Mornhinweg DW, Carver BF, Lane Rayburn A, Nguyen HT** (1987) Photosynthetic differences among *Triticum* accessions at tillering. Crop Sci **27:** 1046–1050
17. **Johnson RC, Nguyen HT, Croy LI** (1984) Osmotic adjustment and solute accumulation in two wheat genotypes differing in drought resistance. Crop Sci **24:** 957–962
18. **Keck RW, Boyer JS** (1974) Chloroplast response to low leaf water potentials. III. Differing inhibition of electron transport and photophosphorylation. Plant Physiol **53:** 474–479
19. **Martin B, Nienhuis J, King G, Schaefer A** (1989) Restriction fragment length polymorphisms associated with water use efficiency in tomato. Science **243:** 1725–1728
20. **Martin B, Thorstenson YR** (1988) Stable carbon isotope composition ($\delta^{13}C$), water use efficiency, and biomass productivity of *Lycopersicon esculentum, Lycopersicon pennellii,* and the F_1 hybrid. Plant Physiol **88:** 213–217
21. **Matthews MA, Boyer JS** (1984) Acclimation of photosynthesis to low leaf water potentials. Plant Physiol **74:** 161–166
22. **Ritchie SW, Nguyen HT, Holaday AS** (1990) Leaf water content and gas-exchange parameters of two wheat genotypes differing in drought resistance. Crop Sci **30:** 105–111
23. **Schonfeld MA, Johnson RA, Carver BF, Mornhinweg DW** (1988) Water relations in wheat as drought resistance indicators. Crop Sci **28:** 526–531
24. **Sharkey TD** (1985) Photosynthesis in intact leaves of C_3 plants: physics, physiology and rate limitations. Bot Rev **51:** 53–105
25. **Stitt M, Wilke I, Feil R, Heldt HW** (1988) Coarse control of sucrose phosphate synthase in leaves: alterations of the kinetic properties in response to the rate of photosynthesis and the accumulation of sucrose. Planta **174:** 217–230
26. **Vassey TL, Quick WP, Sharkey TD, Stitt M** (1991) Water stress, carbon dioxide, and light effects on sucrose-phosphate synthase activity in *Phaseolus vulgaris.* Physiol Plant **81:** 37–44
27. **Vassey TL, Sharkey TD** (1989) Mild water stress of *Phaseolus vulgaris* plants leads to reduced starch synthesis and extractable sucrose phosphate synthase activity. Plant Physiol **89:** 1066–1070
28. **von Caemmerer S, Farquhar GD** (1981) Some relationships between the biochemistry of photosynthesis and the gas exchange of leaves. Planta **153:** 376–387
29. **Walker D** (1987) The Use of the Oxygen Electrode and Fluorescence Probes in Simple Measurements of Photosynthesis. Oxgraphics Limited, Sheffield, UK